Pol. J. Environ. Stud. Vol. 22, No. 5 (2013), 1419-1430

Original Research

Modeling the Effect of Suction Change on a Tropical Black Clay Aquitard during Consolidation

Oluwapelumi O. Ojuri*, Felix N. Okonta

Department of Civil Engineering Science, University of Johannesburg, Johannesburg, Auckland Park, South Africa

Received: 11 July 2012
Accepted: 27 March 2013

Abstract

Consolidation of clayey contaminant barriers such as aquitards (natural aquifer barriers) and landfill liners can be a cause for early breakthrough of contaminants. The general objective of this research was to numerically model the rate of dissipation of pore pressures (soil suction) and change in the void ratio/soil permeability characteristics for a loaded black cotton soil (BCS) aquitard layer and thus evaluate the level of groundwater protection in semi-arid regions with BCS cover. Soil suction change was simulated by varying the degree of saturation of the expansive black clay and applying consolidation pressure. A modified Terzaghi's 1-D consolidation equation was modeled using experimental data from the compressibility characteristics of Black cotton soils for various degrees of saturation. Proposed models for predicting the rate of dissipation of pore pressures and change in void ratio were established for the loaded BCS aquitard layer. The modeling results demonstrate the significance of evaluating the hydraulic properties of soils in relationship to their environments under simulated groundwater table and degree of saturation conditions.

Keywords: excess pore pressures, void ratio, consolidation parameters, groundwater protection, soil suction, natural aquifer barrier

Introduction

Black clays or expansive soils occur widely throughout the world both in temperate and tropical climates. Problems associated with these soils have been reported in Africa, Australia, Europe, India, Israel, South America, Russia, the United States, and some regions in Canada. In many areas of the tropics, especially Africa and India, tropically expansive soils, often known as black cotton soils, are major problematic soils. These soils show very strong swelling and shrinkage characteristics under changing moisture conditions [1]. The problematic northeastern Nigerian soil studied in this research is black cotton soil. In general, black cotton soils derive from basic igneous rocks such as basalts that are rich in feldspars and mafic minerals such as montmorillonites [2]. In Nigeria these soils are found predominantly in the northeastern region of the country, lying within the Chad Basin and partly within the Benue trough (Fig. 1).

The bulk of the black cotton soil deposits in Nigeria are found in the Northeastern States of Borno, Adamawa, Taraba, Gombe, and Bauchi. These soils generally occur in discontinuous stretches as superficial deposits usually not more than 2 meters in thickness, overlain or underlain by sandy sediments [3]. In these areas, erosion superseded by deposition and variations in the characteristics of soils have resulted in variations of infiltration and water-holding capacity.

*e-mail: ojurip@yahoo.com

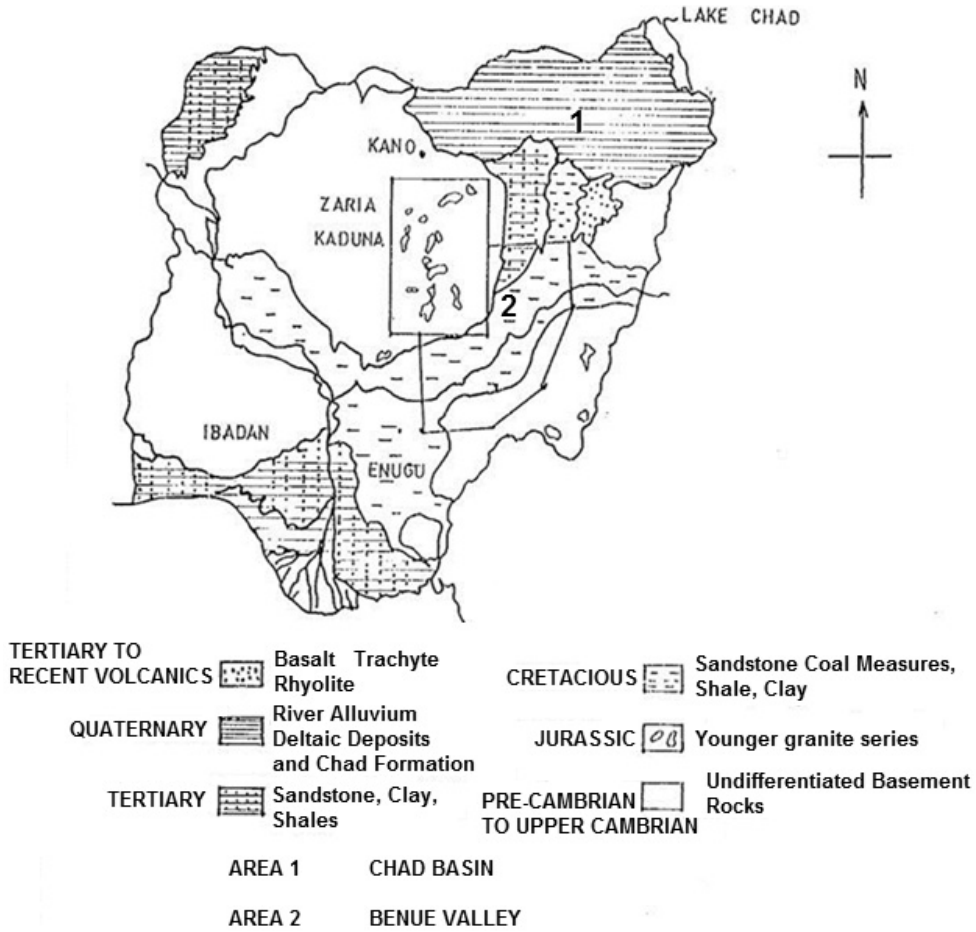

Fig. 1. Geological sketch map of Nigeria (Geological Survey of Nigeria, [24]).

In the Chad basin, the Quaternary Chad formation contains three major aquifers that are separated from one another by various thicknesses of clay. The aquifers are designated the upper, middle, and lower zones, respectively. The upper zone is unconfined or semi-confined, while the middle and lower zones are artesian. Over most of the Benue trough, shallow aquifers tapped by hand-dug wells have the water table generally less than 30 m from the surface [4]. Ijimdiya and Osinubi [5] gave the engineering definition for black cotton soil as dark grey to black soil with a high content of clay, usually over 50% in which montmorillonite is the principal clay mineral and which is commonly expansive. They have the tendency to expand and shrink with changes in moisture, plus appreciable plasticity due to the clay fraction.

The behavior of compacted and natural unsaturated soil is strongly influenced by the state of stress in the pore-water. The pore-water pressure is negative (relative to atmospheric pressure) and varies according to the surrounding micro-climate. A change in negative pore-water pressure in turn produces a change in the volume and shear strength of the soil. An understanding of the effect of changing negative pore-water pressure is important from an engineering standpoint. Negative pore-water pressure relative to the pore-air pressure (i.e. generally atmospheric conditions) is referred to as matric suction [6]. Another component of suction called solute or "osmotic" suction is a function of the salt content of the pore fluid. The sum of the matric suction and solute (osmotic) suction is called total suction.

The prediction of consolidation during the hydrodynamic period in partially saturated soils is more difficult than in saturated soils due to the presence of a second fluid, namely the air. Its presence modifies the phenomenon of consolidation due to changes in (a) effective stress, and (b) coefficient of permeability. A consolidation theory for partially saturated soils should therefore take into account the modified effective stress law, modified coefficient of permeability, and flow of air and water from voids during consolidation. The process of consolidation for a partially saturated soil can be represented by a simple rheological model, [7-9] Fig. 2.

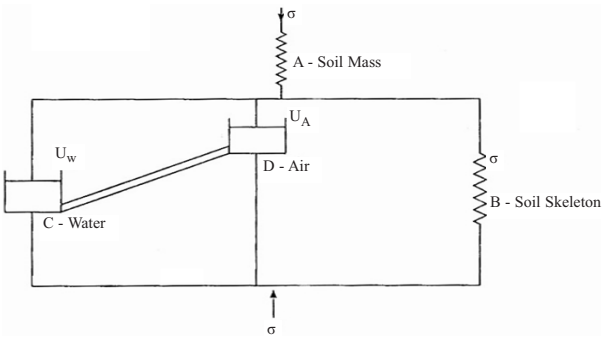

Fig. 2. Rheological model of a partially saturated soil [25].

When a load is applied to the soil mass, certain deformation takes place immediately, depending on the degree of saturation. This corresponds to the deformation of spring A. The load is then taken by the pore fluid resulting in excess pore pressure. The pore fluid flows out under this pressure, and the effective stress on the soil grains increases. The soil mass under increased stress deforms. In the model, the viscous dashpots C and D, and spring B corresponds to water, air and soil skeleton, respectively. The period during which the escape of fluid takes place is called the hydrodynamic period (more correctly the fluid-dynamic period) of consolidation.

The initial hypothesis is that the flow of air and water from soil voids during consolidation (external load application), leading to a change in soil suction and hence the void ratio/hydraulic properties of the unsaturated black cotton soil. Saturated hydraulic conductivity values, depth-to-water table, and other hydrogeological factors are usually considered in evaluating groundwater vulnerability/protection without paying attention to unsaturated soil behavior and the possible effects of external applied loads during unsaturated soil consolidation. The focus advanced in this model study is to apply unsaturated soil principles in modeling an unsaturated black cotton soil aquitard with a view to evaluating levels of groundwater vulnerability/protection for different degrees of saturation under external applied loads. The specific objectives are to extend the theory of 1-D consolidation based on saturated soil assumptions to the analysis of partially saturated soils and derive basic differential equations for 1-D consolidation of partially saturated soils with numerical solutions based on assumed initial and boundary conditions. The objectives include applying partially saturated soil theories to the analysis of black cotton soils as an aquitard (impermeable geologic medium) layer in a semi-arid region and using modeling results, in explaining variation in groundwater vulnerability/protection potential for black cotton soils.

Mathematical Model Formulations

The black cotton deposits occur in a sufficient areal extent to justify a one-dimensional analysis [10]. Lyon Associates, in a wide review of African tropical black clays and black cotton soils, reported that these clays rarely develop thick profiles and quoted maximum depths of about 2 m [11].

The following assumptions are made in the formation of the theory:

i. The flow of air and water is in one direction only. (i.e., in the direction of compression). This corresponds to confined compression of the soil mass.
ii. Pore water and soil grains are incompressible.
iii. The quantity of water in the vapor state is negligible.

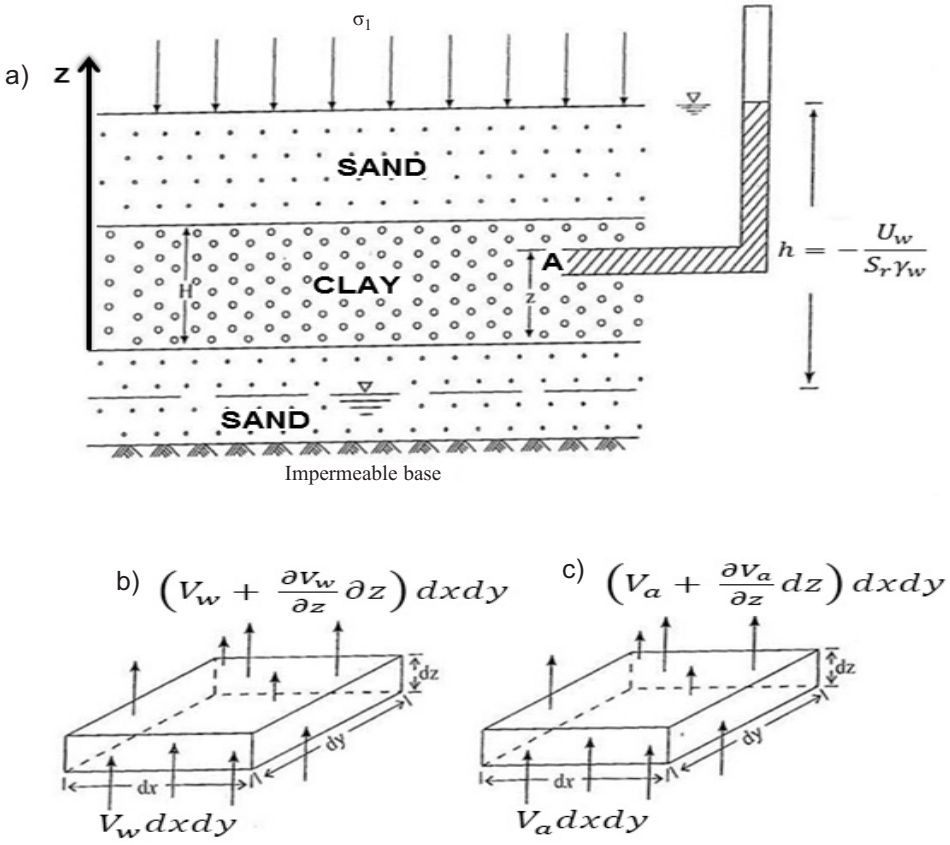

Fig. 3. One-dimensional consolidation for a partially saturated clay layer.
a) Partially saturated clay layer undergoing consolidation.
b) Flow of water at "A" during consolidation
c) Flow of air at "A" during consolidation

iv. Darcy's Law is valid.
v. Void ratio and effective stress are linearly correlated, i.e.

$$de = -a_v \cdot d\sigma^1$$

...where:
e – void ratio
a_v – coefficient of compressibility
σ^1 – effective stress

Fig. 3a shows a layer of partially saturated clay of thickness H located between two highly permeable sand layers. If the clay layer is subjected to increased pressure σ^1, the pore pressure at any point "A" in the clay layer will increase. For one-dimensional consolidation, the fluid will be squeezed out in the vertical direction toward the sand layer. Fig. 3b shows the flow of water through a prismatic element at "A." Similarly, Fig. 3c shows the flow of air through a prismatic element at "A."

For the soil element shown:

(*Rate of outflow of water* + *Rate of outflow of air*) – (*Rate of inflow of water* + *Rate of inflow of air*) = *Rate of volume change*

...i.e.,

$$\left[\left(V_w + \frac{\partial V_w}{\partial z}\partial z\right)dxdy + \left(V_a + \frac{\partial V_a}{\partial z}dz\right)dxdy\right] - [(V_w dxdy + V_a dxdy)] = \frac{\partial V}{\partial t} \quad (1a)$$

...where:
V – volume of soil element
V_w – velocity of flow water in Z direction
V_a – velocity of flow air in Z direction

...or

$$\frac{\partial V_w}{\partial z}dx.dy.dz + \frac{\partial V_a}{\partial z}dx.dy.dz = \frac{\partial V}{\partial t} \quad (1b)$$

Using modified Darcy's law for unsaturated soil [12], we have:

$$V_w = -k_{w(U_a-U_w)} \cdot \frac{\partial h_w}{\partial z}$$

$$h_w = z + \frac{U_w}{\rho_w g}$$

...hence:

$$V_w = -\frac{k_{w(U_a-U_w)}}{\gamma_w} \cdot \frac{\partial U_w}{\partial z} \quad (2)$$

...where:

$k_{w(U_a-U_w)}$ – Unsaturated coefficient of permeability, which is a function of $(U_a - U_w)$

$\frac{U_w}{\rho_w g}$ – Pure-water pressure head

γ_w – unit weight of water

Similarly:

$$V_a = -\frac{k_{w(U_a-U_w)}}{\gamma_a} \cdot \frac{\partial U_a}{\partial z} \quad (3)$$

Substituting (2) and (3) into (1) based on [13]:

$$-\frac{K_{w(U_a-U_w)}}{\gamma_w} \cdot \frac{\partial^2 U_w}{\partial z^2} + \left(\frac{-K_{w(U_a-U_w)}}{\gamma_a} \cdot \frac{\partial^2 U_a}{\partial z^2}\right) = \frac{1}{dx.dy.dz} \cdot \frac{\partial V}{\partial t} \quad (4)$$

During consolidation, the rate of change of volume of the soil element is equal to the rate of change of the volume of the voids, so:

$$\frac{\partial V}{\partial t} = \frac{\partial V_v}{\partial t} = \frac{\partial (V_s + eV_s)}{\partial t} = \frac{\partial V_s}{\partial t} + \frac{V_s \partial e}{\partial t} + e\frac{\partial V_s}{\partial t} \quad (5)$$

...where: V_s – volume of soils, V_v – volume of voids, e – void ratio

But (assuming that soil solids are incompressible),

$$\frac{\partial V_s}{\partial t} = 0$$

...and

$$V_s = \frac{V}{1+e_0} = \frac{dx.dy.dz}{1+e_0}$$

Substitution for $\frac{\partial V_s}{\partial t}$ and V_s in (5) yields

$$\frac{\partial V}{\partial t} = \frac{dx.dy.dz}{1+e_o} \cdot \frac{\partial e}{\partial t} \quad (6)$$

...where: e_0 – initial void ratio

Combining (3.4) and (3.6)

$$-\frac{K_{w(U_a-U_w)}}{\gamma_w} \cdot \frac{\partial^2 U_w}{\partial z^2} + \left(\frac{-K_{w(U_a-U_w)}}{\gamma_a} \cdot \frac{\partial^2 U_a}{\partial z^2}\right) = \frac{1}{1+e_o} \cdot \frac{\partial e}{\partial t} \quad (7)$$

The change of void ratio is due to the increase of effective stress (i.e., decrease of excess pore pressure). Assuming that they are linearly related, we have,

$$\partial e = a_v(\Delta\sigma^1) = a_v \partial[U_a - X(U_a - U_w)] \quad (8)$$

...where: $\Delta\sigma^1$ – the change in effective pressure, a_v – coefficient of compressibility (a_v can be considered to be a constant for a narrow range of pressure increase).

Since, according to [14]:

$$\sigma^1 = \sigma - [U_a - X(U_a - U_w)]$$

...where: σ^1 – effective stress, X – effective stress parameter (determined experimentally), $U_a - U_w$ – soil suction, U_a – pore air pressure.

Combining (7) and (8) gives:

$$-\frac{k_{w(U_a-U_w)}}{\gamma_w} \cdot \frac{\partial^2 U_w}{\partial z^2} + \left(\frac{-k_{w(U_a-U_w)}}{\gamma_a} \cdot \frac{\partial^2 U_a}{\partial z^2}\right) = \frac{-a_v}{1+e_o} \cdot \frac{\partial[U_a - X(U_a - U_w)]}{\partial t}$$

i.e.

$$-k_{w(U_a-U_w)}\left[\frac{1}{\gamma_w}\cdot\frac{\partial^2 U_w}{\partial z^2}+\frac{1}{\gamma_a}\cdot\frac{\partial^2 U_a}{\partial z^2}\right]= -m_v\partial\frac{[U_a-X(U_a-U_w)]}{\partial t}$$

$$\therefore \frac{\partial[U_a-X(U_a-U_w)]}{\partial t}= \frac{k_{w(U_a-U_w)}}{m_v}\left[\frac{1}{\gamma_w}\cdot\frac{\partial^2 U_w}{\partial z^2}+\frac{1}{\gamma_a}\cdot\frac{\partial^2 U_a}{\partial z^2}\right]$$

i.e.

$$\frac{\partial[U_a-X(U_a-U_w)]}{\partial t}= \frac{k_{w(U_a-U_w)}}{\gamma_w m_v}\left[\frac{\partial^2 U_w}{\partial z^2}+\frac{\gamma_w}{\gamma_a}\cdot\frac{\partial^2 U_a}{\partial z^2}\right] \quad (9)$$

...or

$$\frac{\partial[U_a-X(U_a-U_w)]}{\partial t}= C_{v(U_a-U_w)}\left[\frac{\partial^2 U_w}{\partial z^2}+\frac{\partial^2 U_a}{\partial z^2}\cdot\frac{\gamma_w}{\gamma_a}\right] \quad (10)$$

...where: X – effective stress parameter related to degree of saturation, $C_v(U_a - U_w)$ – unsaturated coefficient of consolidation which is a function of $U_a - U_w$.

Rewriting equation (10) we have:

$$\frac{\partial}{\partial t}[[U_a-X(U_a-U_w)]= C_{v(U_a-U_w)}\left[\frac{\partial^2 U_w}{\partial z^2}+\gamma\cdot\frac{\partial^2 U_a}{\partial z^2}\right]$$

...where:

$$\gamma=\frac{\gamma_w}{\gamma_a}$$

...or

$$\frac{\partial}{\partial t}[U_a(1-X)+XU_w]= C_{v(U_a-U_w)}\left[\frac{\partial^2 U_w}{\partial z^2}+\gamma\cdot\frac{\partial^2 U_a}{\partial z^2}\right]$$

$$(1-X)\frac{\partial U_a}{\partial t}+X\frac{\partial U_w}{\partial t}= C\left[\frac{\partial^2 U_w}{\partial z^2}+\gamma\cdot\frac{\partial^2 U_a}{\partial z^2}\right] \quad (11)$$

...where: $C = C_v(U_a - U_w)$

For simplification, X for all practical cases may be taken as equal to the degree of saturation, S_r [15].

∴ Substituting for X in (11) we have:

$$(1-S_r)\frac{\partial U_a}{\partial t}+S_r\frac{\partial U_w}{\partial t}= C\left[\gamma\cdot\frac{\partial^2 U_a}{\partial z^2}+\frac{\partial^2 U_w}{\partial z^2}\right] \quad (12)$$

Consider a model of a partially saturated soil as in Fig. 4.

P_a – force exerted by air on air-solid contact

P_w – force exerted by water on water-solid contact

A_a – area of air-solid contact

A_w – area of water-solid contact

g – acceleration due to gravity

Now, we have that:

$$U_a=\frac{P_a}{A_a} \text{ and } U_w=\frac{P_w}{A_w}$$

A_w is a measure of pore space saturation and is mainly a function of the degree of saturation [16]. From the results of the work by [16, 17], it can be deduced that the degree of saturation of a soil varies inversely as the suction of the soil. This has led to the following assumption relating pore water pressure "U_w" to pore air pressure U_a:

$$U_a=\frac{\alpha}{U_w} \quad (i)$$

Similarly:

$$U_w=\frac{\alpha}{U_a} \quad (ii)$$

...where: α = constant

∴ Substituting the transformation (i) in eq (12) we have:

$$(1-S_r)\cdot\alpha\cdot\frac{\partial\left(\frac{1}{U_w}\right)}{\partial t}+S_r\cdot\frac{\partial U_w}{\partial t}= C[\gamma\cdot\alpha\cdot\frac{\partial^2\left(\frac{1}{U_w}\right)}{\partial z^2}+\frac{\partial^2 U_w}{\partial z^2}$$

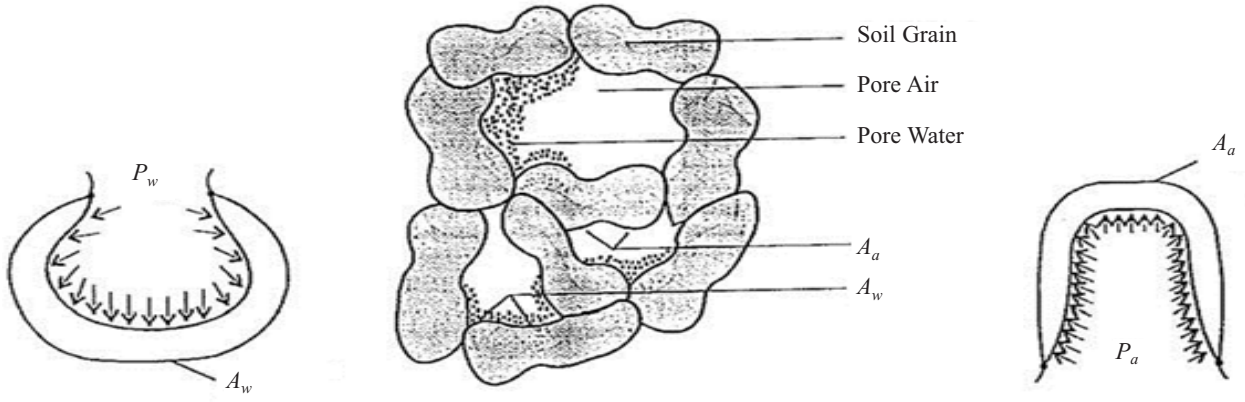

Fig. 4. Model of a partially saturated soil [16].

i.e.

$$(1-S_r)\cdot\alpha\cdot\frac{\partial}{\partial t}\left[\frac{1}{U_w}\right]+S_r\cdot\frac{\partial U_w}{\partial t}=$$
$$C[\gamma\cdot\alpha\cdot\frac{\partial^2}{\partial z^2}\left[\frac{1}{U_w}\right]+\frac{\partial^2 U_w}{\partial z^2} \quad (13)$$

Recall:

$$\frac{d}{dt}\left(\frac{1}{U_w}\right)=\frac{d}{dU_w}\cdot\left(\frac{1}{U_w}\right)\cdot\frac{dU_w}{dt}=-\frac{1}{U_w^2}\cdot\frac{dU_w}{dt}$$
$$\therefore\frac{\partial}{\partial t}\left(\frac{1}{U_w}\right)=-\frac{1}{U_w^2}\cdot\frac{\partial U_w}{\partial t} \quad (iii)$$

also:

$$\frac{d^2}{dz^2}\cdot\left[\frac{1}{U_w}\right]=\frac{d}{dz}\left[\frac{d}{dz}\left(\frac{1}{U_w}\right)\right]=\frac{d}{dz}\left[-\frac{1}{U_w^2}\cdot\frac{dU_w}{dz}\right]$$
$$\frac{d^2}{dz^2}\cdot\left[\frac{1}{U_w}\right]=-\frac{d}{dz}\left(\frac{1}{U_w^2}\right)\cdot\frac{dU_w}{dz}=\frac{1}{U_w^2}\cdot\frac{d^2U_w}{dz^2} \quad (iv)$$

but:

$$\frac{d}{dz}\left(\frac{1}{U_w^2}\right)=\frac{d}{dU_w}\left(\frac{1}{U_w^2}\right)\cdot\frac{dU_w}{dz}=-\frac{2}{U_w^3}\cdot\frac{dU_w}{dz}$$

substituting in (iv), we have:

$$\frac{d^2}{dz^2}\left(\frac{1}{U_w}\right)=\frac{2}{U_w^3}\left(\frac{dU_w}{dz}\right)^2-\frac{1}{U_w^2}\cdot\frac{d^2U_w}{dz^2} \quad (v)$$
$$\left(\frac{dU_w}{dz}\right)^2=U_w.\frac{d^2U_w}{dz^2}$$

Substituting in (v), we have:

$$\frac{d^2}{dz^2}\left(\frac{1}{U_w}\right)=\frac{2}{U_w^2}\cdot\frac{d^2U_w}{dz^2}-\frac{1}{U_w^2}\cdot\frac{d^2U_w}{dz^2}=\frac{1}{U_w^2}\cdot\frac{d^2U_w}{dz^2}$$
$$\therefore\frac{\partial^2}{\partial z^2}\left(\frac{1}{U_w}\right)=\frac{1}{U_w^2}\cdot\frac{\partial^2U_w}{\partial z^2} \quad (vi)$$

Substituting (iii), and (vi) in (13) we have:

$$-\frac{1}{U_w^2}\cdot(1-S_r)\cdot\alpha\cdot\frac{\partial U_w}{\partial t}+S_r\cdot\frac{\partial U_w}{\partial t}=$$
$$C\left[\gamma\cdot\alpha\cdot\frac{1}{U_w^2}\frac{\partial^2U_w}{\partial z^2}+\frac{\partial^2U_w}{\partial z^2}\right]$$

...or:

$$S_r\cdot\frac{\partial U_w}{\partial t}-\frac{1}{U_w^2}\cdot(1-S_r)\cdot\alpha\cdot\frac{\partial U_w}{\partial t}=$$
$$C\left[\frac{\partial^2U_w}{\partial z^2}+\gamma\cdot\alpha\cdot\frac{1}{U_w^2}\frac{\partial^2U_w}{\partial z^2}\right]$$

i.e.

$$\left[S_r-\frac{\alpha}{U_w^2}\cdot(1-S_r)\right]\cdot\frac{\partial U_w}{\partial t}=$$
$$\left[C+\gamma\cdot\alpha\cdot\frac{C}{U_w^2}\right]\cdot\frac{\partial^2U_w}{\partial z^2}$$
$$\frac{\partial U_w}{\partial t}=\frac{\left[C+\gamma\cdot\alpha\cdot\frac{C}{U_w^2}\right]}{\left[S_r-\frac{\alpha}{U_w^2}\cdot(1-S_r)\right]}\cdot\frac{\partial^2U_w}{\partial z^2}$$

Multiply R.H.S by $\frac{U_w^2}{U_w^2}$

$$\frac{\partial U_w}{\partial t}=\left[\frac{CU_w^2+C\cdot\gamma\cdot\alpha}{S_rU_w^2-\alpha(1-S_r)}\right]\cdot\frac{\partial^2U_w}{\partial z^2} \quad (14)$$

Similarly substituting the transformation $U_w=\alpha\cdot\frac{1}{U_a}$ in (12) we have:

$$S_r\cdot\alpha\cdot\frac{\partial\left(\frac{1}{U_a}\right)}{\partial t}+(1-S_r)\frac{\partial U_a}{\partial t}=$$
$$C\left[\alpha\cdot\frac{\partial^2\left(\frac{1}{U_a}\right)}{\partial z^2}+\gamma\cdot\frac{\partial^2U_a}{\partial z^2}\right]$$

$$S_r\cdot\alpha\cdot\frac{\partial}{\partial t}\left[\frac{1}{U_a}\right]+(1-S_r)\frac{\partial U_a}{\partial t}=$$
$$C\left[\alpha\cdot\frac{\partial^2}{\partial z^2}\left[\frac{1}{U_a}\right]+\gamma\cdot\frac{\partial^2U_a}{\partial z^2}\right] \quad (15)$$

Recall from (iii) and (iv):

$$\frac{\partial}{\partial t}\left(\frac{1}{U_a}\right)=-\frac{1}{U_a^2}\cdot\frac{\partial U_a}{\partial t} \quad (vii)$$

...also

$$\frac{d^2}{dz^2}\cdot\left[\frac{1}{U_a}\right]=-\frac{1}{U_a^2}\cdot\frac{d^2U_a}{dz^2} \quad (viii)$$

Substituting (vii) and (viii) in (15):

$$-S_r\cdot\alpha\cdot\frac{1}{U_a^2}\cdot\frac{\partial U_a}{\partial t}+(1-S_r)\frac{\partial U_a}{\partial t}=$$
$$C\left[-\alpha\cdot\frac{1}{U_a^2}\cdot\frac{d^2U_a}{dz^2}+\gamma\cdot\frac{\partial^2U_a}{\partial z^2}\right]$$

...or:

$$\left[(1-S_r)-\frac{\alpha}{U_a^2}\cdot S_r\right]\cdot\frac{\partial U_a}{\partial t}=C\left[\left(-\frac{\alpha}{U_a^2}+\gamma\right)\frac{\partial^2U_a}{\partial z^2}\right]$$
$$\frac{\partial U_a}{\partial t}=\frac{\left[\left(-\alpha\cdot\frac{C}{U_a^2}+C\cdot\gamma\right)\right]}{\left[(1-S_r)-\frac{\alpha}{U_a^2}\cdot S_r\right]}\cdot\frac{\partial^2U_a}{\partial z^2}$$

Multiply R.H.S by $\frac{U_a^2}{U_a^2}$

$$\therefore\frac{\partial U_a}{\partial t}=\frac{\left[\left(-\alpha C+C\cdot\gamma\cdot U_a^2\right)\right]}{\left[(1-S_r)U_a^2-\alpha\cdot S_r\right]}\cdot\frac{\partial^2U_a}{\partial z^2} \quad (16)$$

Relationship between Void Ration and Pore Pressure from eq (8):

$$\partial e=-a_v\partial[U_a-X(U_a-U_w)]$$
$$\partial e=-a_v\partial[(1-X)U_a+XU_w]$$

...or:

$$\frac{\partial e}{\partial t} = -a_v \frac{\partial}{\partial t}[(1-X)U_a + XU_w]$$

$$\frac{\partial e}{\partial t} = -a_v(1-X)\frac{\partial U_a}{\partial t} - a_v \cdot X \cdot \frac{\partial U_w}{\partial t}$$

For simplification X for all practical cases may be taken as equal to S_r:

$$\therefore \frac{\partial e}{\partial t} = -a_v(1-S_r)\frac{\partial U_a}{\partial t} - a_v \cdot S_r \cdot \frac{\partial U_w}{\partial t}$$

$$\frac{\partial e}{\partial t} = -a_v\left[(1-S_r)\cdot\frac{\partial U_a}{\partial t} + \cdot S_r \cdot \frac{\partial U_w}{\partial t}\right]$$

N.B: Coefficient of compressibility $a_v = \frac{\Delta e}{\Delta p}$ (usually disregard the negative sign):

$$\frac{\partial e}{\partial t} = a_v\left[(1-S_r)\cdot\frac{\partial U_a}{\partial t} + S_r \cdot \frac{\partial U_w}{\partial t}\right] \quad (17)$$

The proposed basic differential equations for the theory of one-dimensional consolidation for partially saturated soils are as follows:

$$\frac{\partial U_w}{\partial t} = \left[\frac{CU_w^2 + C\cdot\gamma\cdot\alpha}{S_r U_w^2 - \alpha(1-S_r)}\right]\cdot\frac{\partial^2 U_w}{\partial z^2} \quad (14)$$

$$\frac{\partial U_a}{\partial t} = \frac{[(-\alpha C + C\cdot\gamma\cdot U_a^2)]}{[(1-S_r)U_a^2 - \alpha\cdot S_r]}\cdot\frac{\partial^2 U_a}{\partial z^2} \quad (16)$$

$$\frac{\partial e}{\partial t} = a_v\left[(1-S_r)\cdot\frac{\partial U_a}{\partial t} + S_r \cdot \frac{\partial U_w}{\partial t}\right] \quad (17)$$

Equations (14) and (16) are parabolic and equations with variable coefficients and can be written in a general form as:

$$\frac{\partial U}{\partial t} = K\frac{\partial^2 U}{\partial z^2} \quad (18)$$

...where K≠ a constant.

This diffusion equation can be solved by various schemes/methods, but the implicit scheme has been used because it is more stable.

Numerical Implementation Using Implicit Scheme for Diffusion

The finite difference equivalent of equation (18) can be written as:

$$\frac{{U_i}^{j+1} - {U_i}^{j}}{\Delta t} = a.k\left[\frac{{U^j}_{i+1} - 2{U_i}^j + {U^j}_{i-1}}{(\Delta z)^2}\right] + b.k\left[\frac{{U^{j+1}}_{i+1} - 2{U^{j+1}}_i + {U^{j+1}}_{i-1}}{(\Delta z)^2}\right] \quad (19)$$

...where: $a + b = 1$

The pattern shown in Fig. 5 is used to form the finite difference equation.

From (19)

$${U_i}^{j+1} = {U_i}^j + a.\frac{k\Delta t}{(\Delta z)^2}\left[{U^j}_{i+1} - 2{U_i}^j + {U^j}_{i-1}\right] + b.\frac{k\Delta t}{(\Delta z)^2}\left[{U^{j+1}}_{i+1} - 2{U_i}^{j+1} + {U^{j+1}}_{i-1}\right]$$

Let:

$$r = \frac{k\Delta t}{(\Delta z)^2}$$

$${U_i}^{j+1} = {U^j}_i + arU^j{}_{i+1} - 2arU^j{}_i + arU^j{}_{i-1} + brU^{j+1}{}_{i+1} - 2br{U_i}^{j+1} + brU^{j+1}{}_{i-1}$$

Collecting like terms:

$${U_i}^{j+i} + 2br{U_i}^{j+1} - brU^{j+1}{}_{i+1} - br\,brU^{j+1}{}_{i-1} = {U^j}_i + arU^j{}_{i+1} - 2arU^j{}_i + arU^j{}_{i-1}$$

i.e

$$-brU^{j+1}{}_{i-1} + (1+2br){U_i}^{j+1} - brU^{j+i}{}_{i+1} = {U^j}_i + ar\left(U^j{}_{i+1} - 2U^j{}_i + U^j{}_{i-1}\right) \quad (20)$$

Equation (20) can be written as:

$$-AU^{j+1}{}_{i-1} + BU^{j+1}{}_i - CU^{j+1}{}_{i+1} = D^j \quad (21)$$

...where:

$A = br$

$B = 1 + 2br$

$C = br$

$$D^j = {U^j}_i + ar(U^j{}_{i+1} - 2U^j{}_i + U^j{}_{i-1})$$

Suppose:

$${U_i}^{j+i} = \alpha_i U^{j+1}{}_{i-1} + \beta_i \quad (22)$$

$$\rightarrow {U_{i+1}}^{j+i} = \alpha_{i+1}U^{j+1}{}_i + \beta_{i+1} \quad (23)$$

Then equation (21) becomes:

$$-A\alpha_{i+1}{U_i}^{j+1} - \beta_{i+1}A + B{U_i}^{j+1} - C{U_{i-1}}^j = D^j$$

$$\rightarrow (B - A\alpha_{i+1}){U_i}^{j+1} - C{U_{i-1}}^j = D^j + \beta_{i+1}.A$$

$$\rightarrow {U_i}^{j+1} = \frac{C}{B - A\alpha_{i+1}}{U_{i-1}}^{j+1} + \frac{D^j + \beta_{i+1}.A}{B - A\alpha_{i+1}} \quad (24)$$

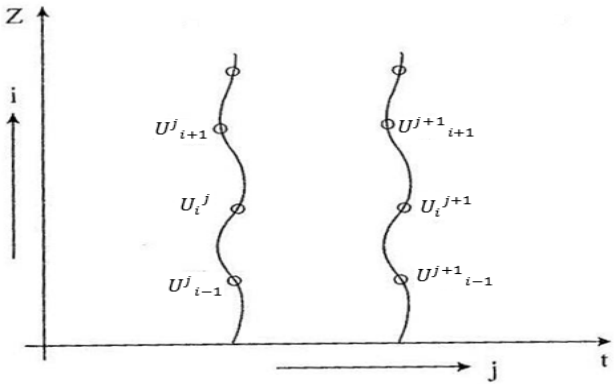

Fig. 5. Finite-difference grid pattern.

Now compare equations (22) and (24):

$$\alpha_i = \frac{C}{B - A\alpha_{i+1}}$$

$$\rightarrow \beta_i = \frac{D^j + \beta_{i+1}.A}{B - A\alpha_{i+1}}$$

Using a given boundary condition at the top (Fig. 6), we can obtain the value for α_{m-i} from equations (22), hence calculate the parameters (α, β) at all levels from the top of the surface using equations (25) and (26)

The assumed initial and boundary conditions are as follows:

$$U = U_o = -S_r\gamma_w z \quad \text{for} \quad 0 \leq z \leq 1 \quad \text{at} \quad t = 0$$

U=0 when z=0 and 1 for all 't'

In our case, the boundary conditions are given as:

U=0 when z=0 and 1 for all 't'

Since:

$$U_i^{j+i} = \alpha_i . U_{i-1}^{j+1} + \beta_i \qquad (22)$$

If U=0 at the top

$\rightarrow U_m$=0

i.e. α_m=0, β_m=0

Hence we compute our parameters (α, β) from top to bottom and the values of U from bottom to top.

To solve equation (17),

Recall:

$$\frac{\partial e}{\partial t} = a_v\left[(1 - S_r)\cdot\frac{\partial U_a}{\partial t} + S_r \cdot \frac{\partial U_w}{\partial t}\right]$$

$$\rightarrow \frac{\partial e}{\partial t} = a_v(1 - S_r).\frac{\partial U_a}{\partial t} + a_v S_r.\frac{\partial U_w}{\partial t}$$

Equation (18) can be written in general form as

$$\frac{\partial e}{\partial t} = N_a.\frac{\partial U_a}{\partial t} + N_w.\frac{\partial U_w}{\partial t} \qquad (27)$$

The finite difference equivalent for (27) is as follows:

$$\frac{{e_i}^{j+1} - {e_i}^j}{\Delta t} = N_a\left[\frac{{U_a}^{j+1}{}_i - {U_a}^j{}_i}{\Delta t}\right] + N_w\left[\frac{{U_w}^{j+1}{}_i - {U_w}^j{}_i}{\Delta t}\right]$$

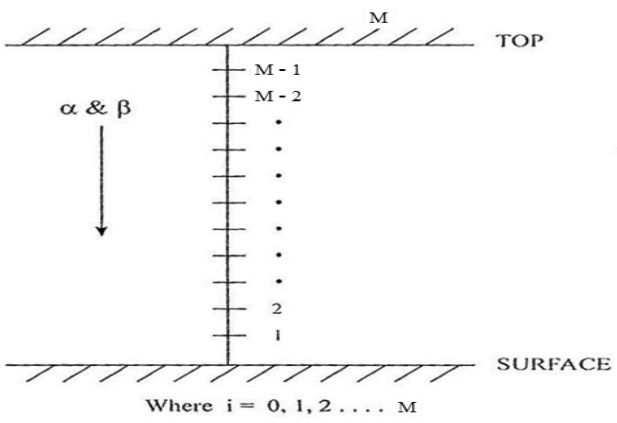

Fig. 6. Grid points and boundary values.

Table 1. Summary of input data for the model.

Case No.	S_r	c_v (cm²/sec)	a_v (m²/KN)
1	0.2	5.3×10^{-3}	0.7×10^{-4}
2	0.4	4.6×10^{-3}	1.29×10^{-4}
3	0.6	4.3×10^{-3}	1.72×10^{-4}
4	0.8	9.98×10^{-3}	1.76×10^{-4}
5	1.0	1.07×10^{-2}	2.7×10^{-4}

i.e

$$e^{j+1}{}_i = e^j{}_i + N_a\left[{U_a}^{j+1}{}_i - {U_a}^j{}_i\right] + N_w\left[{U_w}^{j+1}{}_i - {U_w}^j{}_i\right] \qquad (28)$$

Results and Discussion

The proposed basic differential equations for the theory of one-dimensional consolidation for partially saturated soils was solved using an implicit method of numerical analysis, imposing the assumed initial and boundary conditions. The model was tested using the experimental values of the degree of saturation and various soil parameters obtained from compressibility and suction tests on the black cotton soil in Table 1 [18]. This numerical technique was used for the solution of equations (14), (16), and (17). Constants and parameters specified for the model are:

$\gamma_w = 10KN/m^3$, $\gamma_a = 0.013KN/m^3$

$\gamma = \frac{\gamma_w}{\gamma_a} = \frac{10}{0.013} = 770$, $\alpha = 1.0$ (assumed)

H = 100 units, $\Delta Z = 1$, $\Delta t = 2secs$

A summary of the input data is shown in Table 1.

The computer program is written in Fortran 90, and the plotting of the results was done with the MATLAB package.

Six cases (soil saturation scenarios), namely Case 1 (S_r = 20%), Case 2 (S_r = 40%), Case 3 (S_r = 60%), Case 4 (S_r = 80%), Case 5 (S_r = 100%), and Case 5s (Special case for S_r = 100% with longer simulation period) were simulated and the profiles and times series for the pore pressures and void ratio plotted. Only the plots and time series for cases 1, 2, 5, and 5 s are presented in Figs. 7 to 10. Figs. 7a to 10a show the plots for the profiles of U_w, U_a, and e.

For Case 1 (Sr = 20%) soil suction dropped abruptly from about 30,000 kPa to zero at the end of consolidation, and the change in void ratio (Δe) was 0.25 (Fig. 7a). It took 0.25 days (6 hours) for the pore pressure to dissipate to zero for the mid height plot in Fig. 7b. For Case 2 (S_r = 40%), soil suction dropped from about 6,000 kPa to zero at the end of consolidation, and the change in void ratio (Δe) was 0.40 (Fig. 8a). It took 0.5 days (12 hours) for the pore pressure to dissipate to zero for the mid-height plot in Fig. 8b. For Case 3 (S_r = 60%), soil suction dropped from about 1,000 kPa to zero at the end of consolidation, and the change in void ratio was 0.55. It took 0.8 days (19.2 hours)

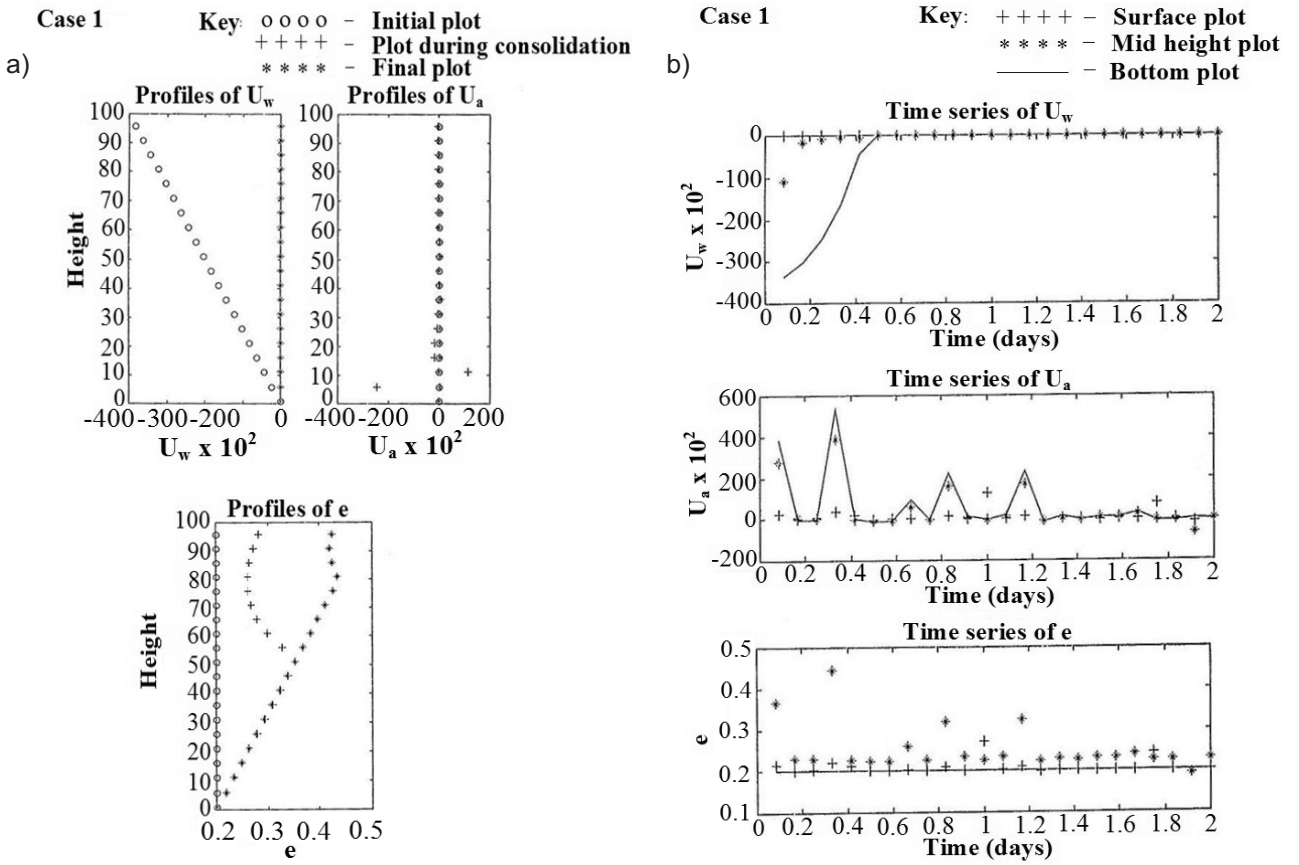

Fig. 7. a) Profiles of U_w, U_a (kPa), and e for S_r = 20%, c_v = 5.3×10^{-3} cm^2/sec, a_v = 0.7×10^{-4} m^2/kN, ftime, simulation period = 172,800 secs. b) Time series of U_w, U_a (kPa), and e for S_r = 20%, c_v = 5.3×10^{-3} cm^2/sec, a_v = 0.7×10^{-4} m^2/kN, ftime, simulation period = 172,800 secs.

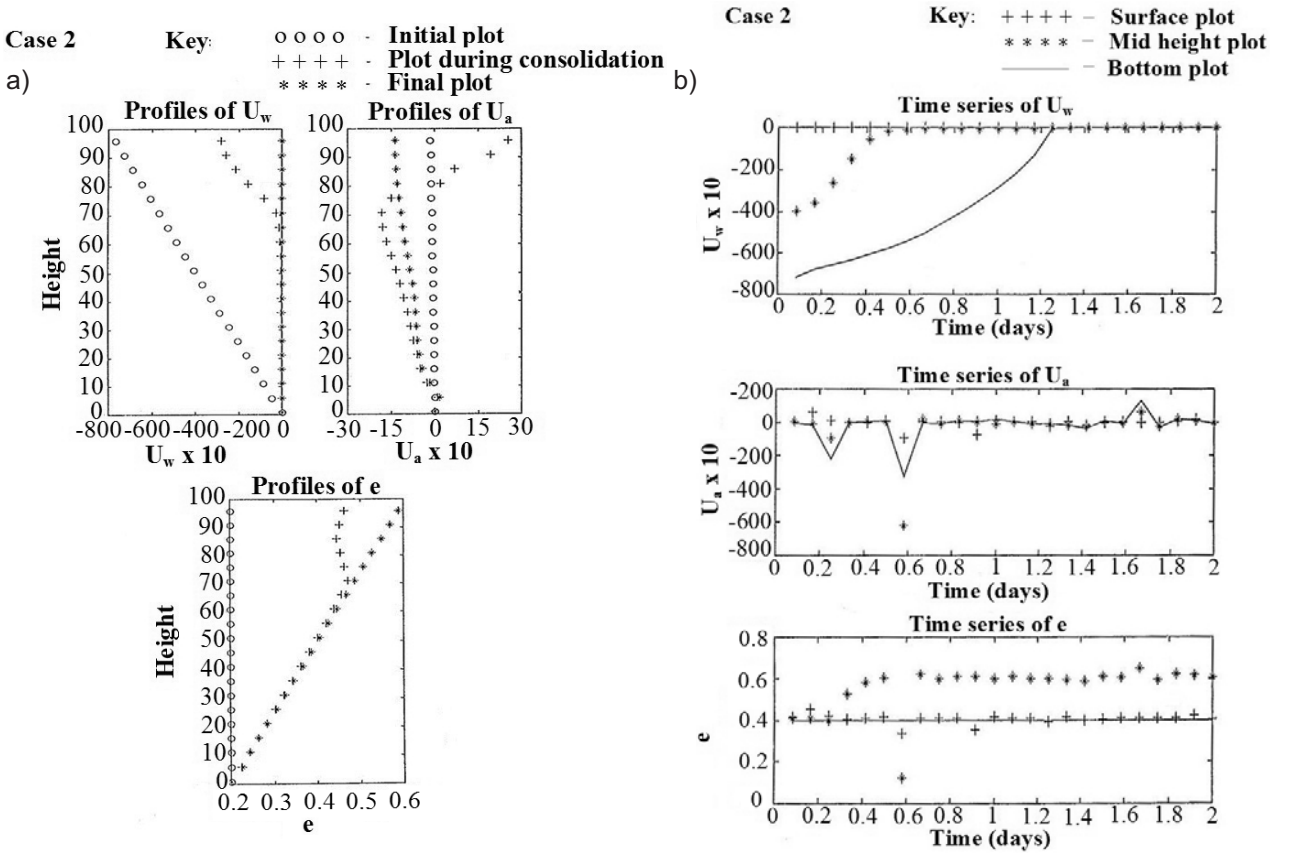

Fig. 8. a) Profiles of U_w, U_a (kPa), and e for S_r = 40%, c_v = 4.6×10^{-3} cm^2/sec, a_v = 1.29×10^{-4} m^2/kN, ftime, simulation period = 172,800 secs. b) Time series of U_w, U_a (kPa), and e for S_r = 40%, c_v = 4.6×10^{-3} cm^2/sec, a_v = 1.29×10^{-4} m^2/kN, ftime, simulation period = 172,800 secs.

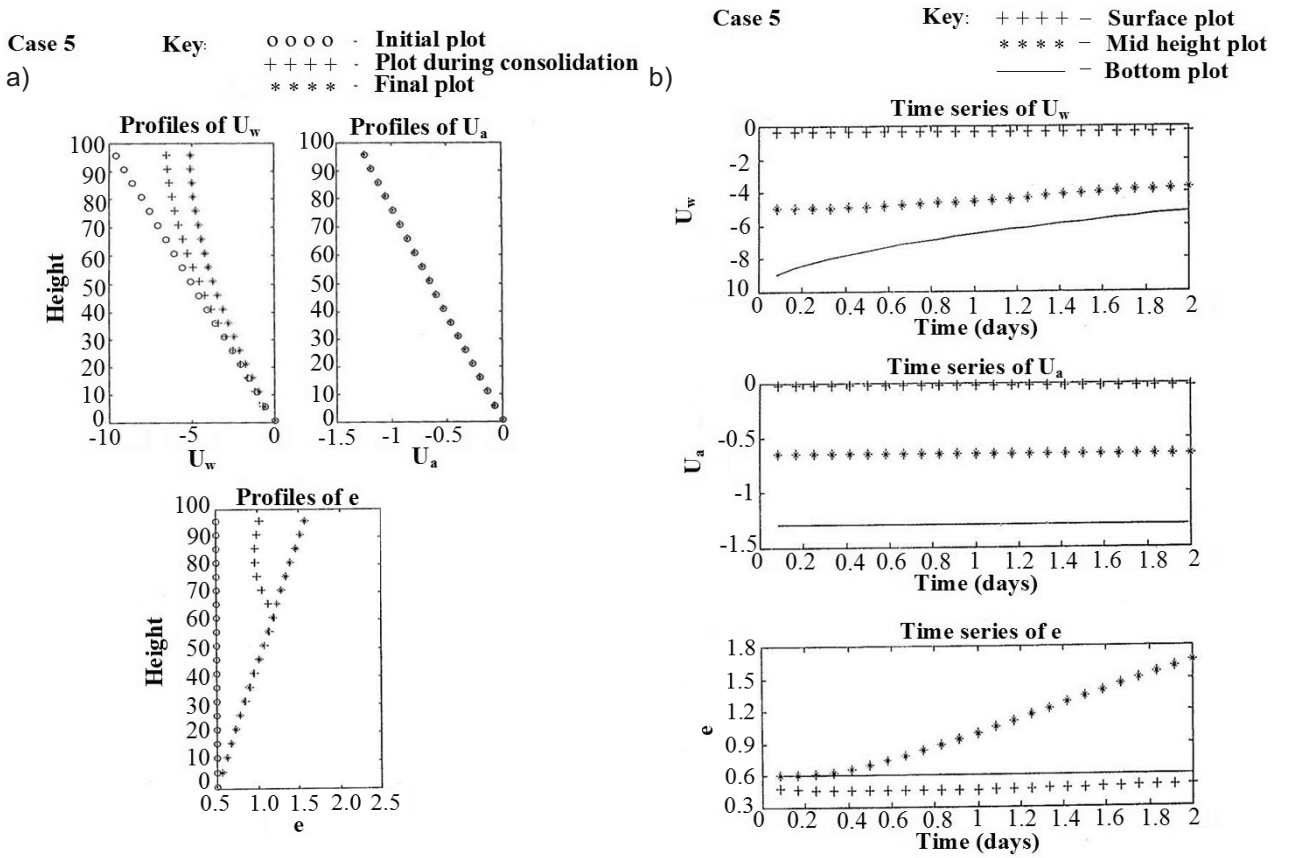

Fig. 9. a) Profiles of U_w, U_a (kPa), and e for S_r = 100%, c_v = 1.07×10^{-2} cm^2/sec, a_v = 2.7×10^{-4} m^2/kN, ftime, simulation period = 172,800 secs.
b) Time series of U_w, U_a (kPa), and e for S_r = 100%, c_v = 1.07×10^{-2} cm^2/sec, a_v = 2.7×10^{-4} m^2/kN, ftime, simulation period = 172,800 secs.

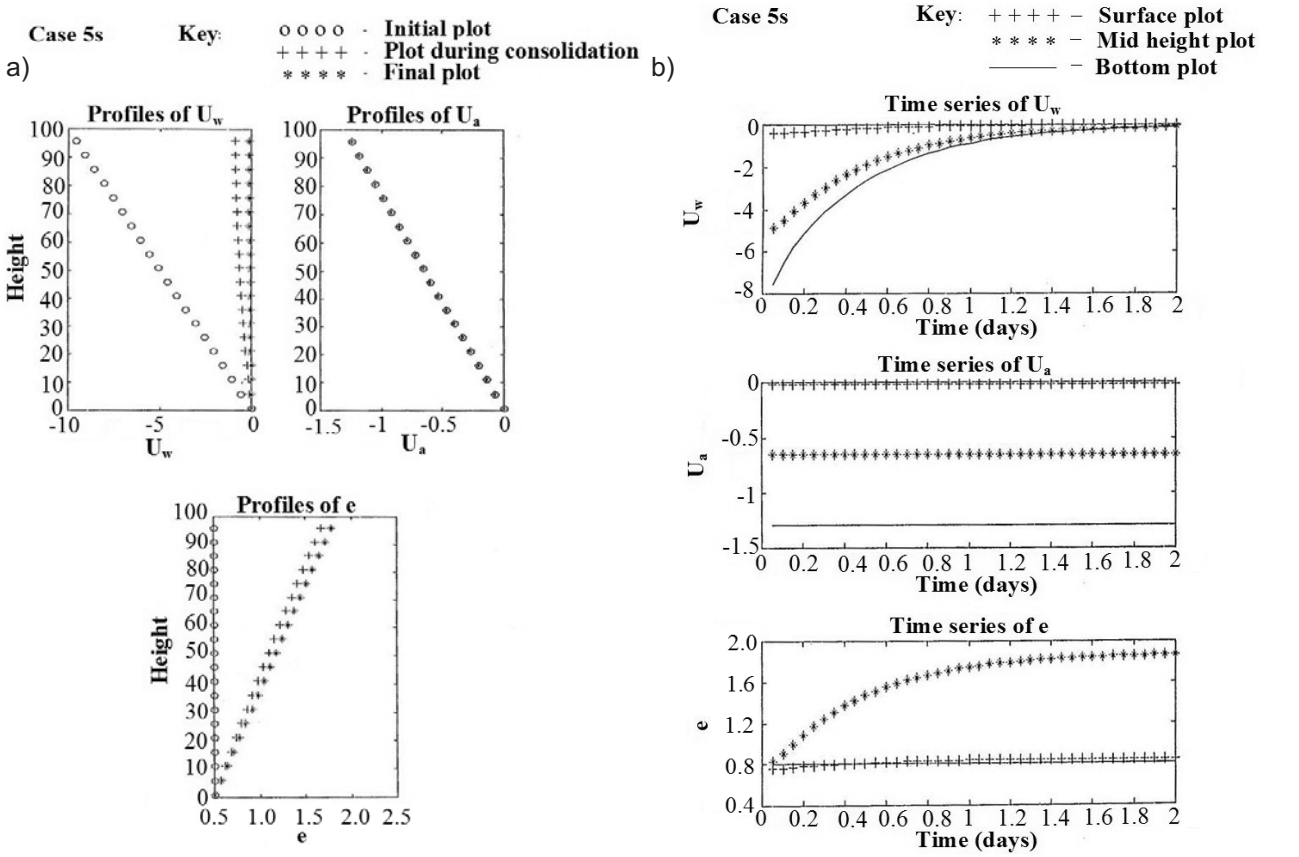

Fig. 10. a) Profiles of U_w, U_a (kPa), and e for S_r = 100%, c_v = 1.07×10^{-2} cm^2/sec, a_v = 2.7×10^{-4} m^2/kN, ftime, simulation period = 172,8000 secs.
b) Time series of U_w, U_a (kPa), and e for S_r = 100%, c_v = 1.07×10^{-2} cm^2/sec, a_v = 2.7×10^{-4} m^2/kN, ftime, simulation period = 172,8000 secs.

for the pore pressure to dissipate to zero for the mid-height plot. For Case 4 (S_r = 80%), soil suction dropped from about 20 kPa to zero at the end of consolidation, and the change in void ratio was 0.80. It took 0.9 days (21.6 hours) for the pore pressure to dissipate to zero for the mid-height plot. For Case 5 (S_r = 100%), soil suction dropped from about 10 kPa to zero at the end of consolidation, and the change in void ratio was 1.10 (Fig. 9a). It took more than 2 days for the pore pressure to dissipate to zero for the mid-height plot in Fig. 9b. For Case 5s (S_r = 100%), simulated for a longer period, soil suction dropped from about 10 kPa to zero at the end of consolidation, and the change in void ratio was 1.40 (Fig. 10a). It took more than 16 days for the pore pressure to dissipate to zero for the mid height plot in Fig. 10b. Change in soil suction for this expansive soil has a significant effect on the void ratio, which is a direct indication of its effect on the soil skeleton. Generally, from the results of the suction profiles and time series plots, changes in void ratio are less for high soil-suction changes, while changes in void ratio are more for low soil-suction changes. The increase in void ratio with the degree of saturation together with the increase in the coefficient of consolidation (c_v) and the coefficient of compressibility (a_v) in Table 1 would lead to increased permeability for the black cotton soil aquitard with increasing degree of saturation and decreasing soil suction [19-22].

It can be seen that, except at the initial stage, the plots follow a parabolic pattern during the process of consolidation. The rate of reaching complete saturation also is seen to be decreasing with increasing height from the bottom as expected, depending on the degree of saturation. The suction profiles show that the farther away from the water table, the slower the rate of dissipation of excess pore pressure. The profiles for the different degrees of saturation in Figs. 7a to 9a are for a simulation period of two days. The profile for 'U_w' and 'U_a' at 100% saturation shown in Fig. 10a and the corresponding time series in Fig. 10b is for a simulation period of 20 days. This is the result for case 5s, which has essentially the same input data as case 5 at 100% saturation, except that it was allowed a longer simulation period. It was observed that all the excess pore water pressure dissipated after a simulation period of 20 days. This confirms that the hydrodynamic period of consolidation for a saturated soil is much greater than that of the partially saturated soil. As the negative pore water pressure (suction) decreases and tends toward zero, voids ratio '*e*' is seen to be increasing, implying that essentially suction is responsible for the swell in black cotton soil when it comes into contact with water.

Figs. 7b to 10b show the time series of U_w, U_a, and e at the bottom, mid-height, and surface of the soil layer. The curves are plotted for different degrees of saturation. As expected, the lower the degree of saturation, the faster the rate of change of the pore water and pore air pressures. This explains the precarious effect that exposure to little rain can have on aquitard soil cover around water supply wells with black cotton soil, and the high swell-shrink characteristics of the soil. The time series for pore water pressure U_w and pore air pressure U_a at different points along the height of the clay layer for a simulation period of 2 days are shown in Figs. 7b to 9b. It is interesting to note that the rate of change in pore water pressure increases with decreasing degree of saturation. Experimental and theoretical trends for the variation in pore water and pore air pressures with degree of saturation are in reasonably good qualitative agreement for the partially saturated black cotton soil. In general, soil suction (negative pore water pressure) decreases and tends to zero as the consolidation period expires for the partially saturated soil.

In Jimeta metropolis, which is in the Northeastern States of Adamawa, Nigeria, chloride concentrations in most sampled wells were higher than the 200.0 mg/l recommended highest desirable value [23]. The total dissolved solid (TDS) values were also higher than the recommended maximum of 500.0 mg/l. It was concluded that shallow wells in the Jimeta area had been contaminated [4]. It was alerted that incipient contamination of deeper aquifers caused by leakage of shallow groundwater beneath the metropolis will eventually occur.

Conclusion

Change in the void ratio, which was between 0.25 and 0.40 for the case of 20% and 40% saturation when soil suction was between 30,000 kPa and 6000 kPa, increased to between 1.1 and 1.4 for 100% saturation when soil suction was 10kPa. The change of matric suction exerts a significant effect on the soil skeleton for this tropical expansive clay. This implies that essentially soil suction is responsible for the swelling behavior in this soil. For the hydrodynamic period of consolidation this was between 0.25 days and 0.5 days for 20% and 40% saturation, it increased to about 16 days for 100% saturation. Rapid change in soil suction brought about by change in the degree of saturation or water content and applied external load during soil consolidation would adversely affect the level of protection a black cotton soil aquitard can give to the underlying aquifer. The results show that the farther away from the water table, the slower the rate of dissipation of excess pore pressure. These data demonstrate the significance of evaluating the fundamental properties of soils in relationship to their environment under the simulated groundwater table and degree of saturation conditions. The theoretical and experimental studies confirm that the period for complete consolidation increases as the degree of saturation increases as expected, with 100% degree of saturation giving the longest hydrodynamic period. Increasing the water supply hand-dug well apron coverage area to minimize variations in soil moisture for the aquitard (soil cover in the immediate vicinity of water supply wells) during the dry and wet (rainy) seasons will reduce the risk of groundwater contamination.

Acknowledgements

Prof. Adeyeri J. B., Professor of Geotechnical Engineering is highly appreciated for his supervisory role during the course of this research.

Abbreviations

U_w – pore water pressure, kN/m^2
U_a – pore air pressure kN/m^2
e – void ratio
c_v – coefficient of consolidation, cm^2/min
τ – shear stress, kN/m^2
σ – normal stress kN/m^2
c – cohesion, kN/m^2
ϕ – angle of internal friction
U_a–U_w – soil suction pF
a_v – coefficient of compressibility
S_r – degree of saturation, %
w – moisture content, %
C_c – compression index
C_s – swell index

References

1. DANIEL T. P. Influence of drainage condition on shear strength parameters of expansive soils. Unpublished M. Sc. thesis Addis Ababa University, Addis Ababa, Ethiopia, pp. 33, **2004**.
2. OSINUBI K.J., THOMAS S. A. Influence of compactive efforts on bagasse ash treated black cotton soil. Nigerian Journal of Soil and Environmental Research, **7**, 92, **2007**.
3. IORLIAM A. Y., AGBEDE I. O., JOEL M. Effect of cement kiln dust (CKD) on some geotechnical properties of black cotton soil (BCS). Electronic Journal of Geotechnical Engineering, **17**, (H), **2012**. [online] http://www.ejge.com/2012/Ppr12.088alr.pdf (Accessed 14 June 2012).
4. ADEKEYE J. I. D., ISHAKU J. M. Groundwater contamination in shallow aquifers of Jimeta metropolis, Adamawa State, N. E. Nigeria. Zuma Journal of Pure and Applied Sciences, **6**, (1), 150, **2004**.
5. IJIMDIYA, T. S., OSINUBI, K. J. Attenuative capacity of compacted black cotton soil treated with bagasse ash. Electronic Journal of Geotechnical Engineering, **16**, (D), **2011** [online] http://www.ejge.com/2011/Ppr11.029/Ppr11.029.pdf (Accessed 7 January 2012).
6. KARUBE D., KAWAI K. The role of pore water in the mechanical behavior of unsaturated soils. Geotechnical and Geological Engineering, **19**, 211, **2001**.
7. GAO S., WANG J., ZHOU X. Solution of a rigid disk on saturated soil considering consolidation and rheology. Journal of Zhejiang University SCIENCE, **6A**, (3), 222, **2005**.
8. XIE K., XIE X., LI X. Analytical theory for one-dimensional consolidation of clayey soils exhibiting rheological characteristics under time-dependent loading. Int. J. Numer. Anal. Met., **32**, (14), 1833, **2008**.
9. TI K. S., HUAT B.B.K, NOORZAEI J., JAAFAR M.S., SEW G. S. A review of basic soil constitutive models for geotechnical application. Electronic Journal of Geotechnical Engineering, **14**, (J), **2009** [online] http://www.ejge.com/2009/Ppr0985/Ppr0985ar.pdf (Accessed 14 June 2012).
10. LEWIS T. W., PIVONKA P., SMITH D. W. Theoretical investigation of the effects of consolidation on contaminant transport through clay barriers. Int. J. Numer. Anal. Met., **33**, 95, **2009**.
11. OLA S.A. Geotechnical properties of Nigerian black cotton soils.' In Ola S.A. (Eds.), Tropical soils of Nigeria in engineering practice A.A. Balkerma, Rotterdam, pp. 85-101, **1983**.
12. NARASIMHAN T. N. Darcy's law and unsaturated flow. Vadose Zone Journal, **3**, 1059, **2004**.
13. FREDLUND D. G., RAHARDJO Soil Mechanics Principles for Highway Engineering in Arid Regions. Transportation Research Board, A2L06 Session, **1987**.
14. NUTH M., LALOUI L. Effective stress concept in unsaturated soils: Clarification and validation of a unified framework. Int. J. Numer. Anal. Met., **32**, 771, **2008**.
15. KHALILI N., GEISER F., BLIGHT G.E. Effective stress in unsaturated soils: review with new evidence. International Journal of Geomechanics, **4**, (2), 115, **2004**.
16. LU L., LIKOS W. J. Suction stress characteristic curve for unsaturated soil. Journal of Geotechnical and Geoenvironmental Engineering, **132**, (2), 131, **2006**.
17. FREDLUND D. G. Unsaturated Soil Mechanics in Engineering Practice. Journal of Geotechnical and Geoenvironmental Engineering, **132**, (3), 286, **2006**.
18. OJURI O. O. Effect of soil suction on the compressibility and strength of North-Eastern Nigerian black cotton soil. Electronic Journal of Geotechnical Engineering, **17**, (G), **2012**. [online] http://www.ejge.com/2011/Ppr11.029/Ppr11.029.pdf (Accessed 5 May 2012).
19. NAGARAJ T. S., PANDIAN N. S., NARASIMHA RAJU P. S. R. Stress state – Permeability relationships for fine-grained soils. Geotechnique, **43**, (2), 333, **1993**.
20. SIDDIQUE A., SAFIULLAH A. M. M. Permeability characteristics of reconstituted Dhaka clay. Journal of Civil Engineering Division the Institution of Engineers, Bangladesh, **CE23**, (1), 103, **1995**.
21. HORPIBULSUK S., YANGSUKKASEAM N., CHINKULKIJNIWAT A., DU Y. J. Compressibility and permeability of Bangkok clay compared with kaolinite and bentonite. Appl. Clay Sci., **52**, 150, **2011**.
22. XU G., GAO Y., JI F., CAO Y. Permeability coefficients of dredged slurries at high void ratio. Applied Mechanics and Materials, **170-173**, 1269, **2012**.
23. WORLD HEALTH ORGANIZATION. Guideline for drinking water quality, Health Criteria and other information. 2nd Edition, WHO, Geneva. pp. 281-283, **1998**.
24. NGSA. Geological map of Nigeria, from Nigerian Geological Survey Agency, Abuja, Nigeria, **2004**.
25. OKUBO S., FUKUI K., GAO X. Rheological behaviour and model for porous rocks under air-dried and water-saturated conditions. The Open Civil Engineering Journal, Bentham Open, 1874-1495/08, 2, 88-98, **2008**.